Theoretical analysis of air bending at high temperature

*J.A. Canteli, J.L. Cantero, M.H. Miguélez**

Department of Mechanical Engineering, University Carlos III of Madrid, Av. Universidad 30, 28911 Leganés (Madrid), Spain

Keywords:
Air bending
High temperature
Sheet metal forming
Modelling
Springback

This paper is focused on the theoretical analysis of air bending at high temperature. A thermo-mechanical model able to predict temperature distribution and main bending parameters is developed. Thermal model assumes local heating of the sheet along bend length and is based in previous numerical model. The influence of temperature in mechanical properties of the sheet is taken into account with temperature dependent parameters of constitutive equation. Mechanical model is formulated in order to satisfy industrial requirements. Desired geometry of the piece fixes final bending angle after unloading, so this parameter is the input of the model. An iterative calculation process is used to solve presented equations obtaining curvature, sheet shape, contact force and springback. These parameters are very important in industrial processes, allowing establishment of punch displacement and maximum force to make the desired workpiece. Other results may be obtained from this model: moment distribution, maximum stress and strain. These results are related to important features of the actual process, like tools design and formability limits of the sheet.

1. Introduction

Sheet metal forming processes are commonly used in industry. Decreasing batch sizes in sheet metal part manufacturing, higher accuracy demands and shorter lead times, call for flexible processes (de Vin et al., 1996). On the other hand, advanced materials recently used in structural applications (like high resistance steels in automotive applications), present reduced formability (Hsu et al., 2002). Sheet metal forming processes are usually carried out at room temperature (except laser processes that involves sheet heating). Forming at elevated temperature could solve, in part, associated problems, because of increased formability of the sheet, reduced springback and decrease in maximum process force, that allow forming thicker sheet with the same equipment (Canteli, 2003).

Bending is one of the most usual forming operations. Air bending presents several advantages when compared with bottoming: potential for numerical control of bend angles and a reduced need for tool changes. In air bending a sheet is bent on a press brake with the use of a punch and a die. The punch is lowered to a pre-calculated position, not completely, so it is possible to obtain different bend angles with the same set of tools. However it should not be underestimated the complexity of the process (de Vin, 2001). Process models based in realistic assumptions, should be established in order to predict punch penetration and bend angle, according to actual process conditions.

During bending operations, previous local heating of the sheet along the bend length would provide some advantages, as is shown firstly. High temperature in a narrow area around bend length involves less maximum force, reduced springback and improved bendability. Avoiding complete heating of the sheet, oxidation in an extended surface is prevented, energy cost is lower and furnace dimensions are smaller than in the case of introduction of the sheet in the furnace (Canteli et al., 2006).

* *Corresponding author*. Tel.: +34 91 624 94 02; fax: +34 91 624 94 30.
E-mail address: mhmiguel@ing.uc3m.es (M.H. Miguélez).

Several authors have developed models for air bending processes. Simple models assume that cross-section of a bent sheet consists of a circular part and two straight legs. Due to the large number of simplifying assumptions, results are not very accurate (de Vin, 2000). Three section models consider three types of deformed sections in a bent sheet under loading conditions: a wrap-around zone under the punch, two elasto-plastically deformed zones in which the local radius varies and two elastically deformed sections. Models based on the wrap-around assumption have a limited application (de Vin, 2000). Another model, Anokye-Siribor and Singh (2000) assume a parabolic sheet shape under the punch to make calculations, taking into account effective sheet thickness and neutral axis displacement, and is based on experimental conclusions obtained from the physical modelling of the bending process by the author. On the other hand Asnafi (2000) proposed a model with no assumptions about the shape of the sheet. Sheet curvature was related with moment in each section due to a estimated bending force. Model proposed in this paper is based in part in Asnafi's work. Differences are introduced in the treatment of the bending force and in the thermal analysis of distribution of temperature in the sheet, as it will be shown later.

In present work air bending process at local elevated temperature, along bend length, is analysed. Firstly, a new analytical model of air bending process is developed taking into account changes in mechanical behaviour due to temperature distribution. Since constitutive equation of the material sheet as a function of temperature, should be included, temperature distribution is calculated developing a model for thermal problem. This model is based in the device projected to validate the model with experimental work. Previous numerical analysis of temperature distribution was carried out in order to establish realistic hypothesis in analytical model.

The thermo-mechanical model developed in this paper does not assume a known shape of the sheet. From equilibrium conditions, relations between moment and curvature and constitutive equations, sheet curvature is calculated in an iterative process. Mechanical properties of material are dependent on sheet temperature, therefore the temperature distribution should be previously established. Results obtained from this thermo-mechanical model are presented in this paper.

2. Temperature distribution

As is well known, material's mechanical behaviour depends on temperature. When a metal sheet is locally heated along bend length a temperature distribution is generated in the sheet. This distribution depends on heating parameters, material properties and sheet geometry.

Experimental set up, designed and fabricated in order to validate the model, determine heating parameters. Projected heating device consists of two electrical resistances, located in a vertical plane containing bend line, under and over the sheet along the bend length. Heating parameters are time of heating t, resistance power P, contact force between resistance and sheet a, and resistance radius R.

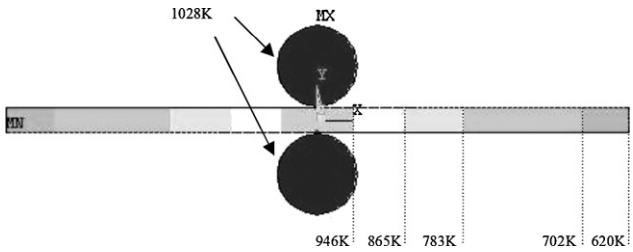

Fig. 1 – Numerical model used to predict temperature distribution (K).

Firstly, some assumptions should be made. They are based in previous finite element analysis of the thermal problem. This numerical model was developed in ANSYS (2000). The sheet is divided in elements Δx width, 1 m length, and e thick.

Numerical modelization showed:

- Temperature was constant in plane YZ, so only variation of temperature in X direction is considered. Axis Z is parallel to bend length, plane XZ is coincident with middle surface of undeformed sheet, axis Y completes reference system.
- Temperature is not linear with X coordinate, so temperature gradient in this direction, is not constant. However, thermal induced stresses were not significant, because temperature non-linearity with X is not very pronounced.
- Heating time to permanent conditions is less than 20 min for parameters ranges studied in this work.

Thermal constants not available from technical literature were also obtained from previous numerical simulation. Fig. 1 shows unidirectional temperature distribution in the sheet resulting from numerical simulation.

Assuming these hypotheses, thermal model was formulated as represented in Fig. 2. Each element is ΔX width and 1 m length, and e thick. Uniform temperature T_n in each element is assumed. Thermal flows in element n are represented in Fig. 3 being:

- Conduction flows from element $n-1$ and to element $n+1$ ($E_{\text{cond } n-1}$, $E_{\text{cond } n}$).
- Convection flows from element n to air (E_{conv}).
- Radiation flows from each resistance to element n and from element n to air ($E_{\text{radressheet}}$, E_{rad}).

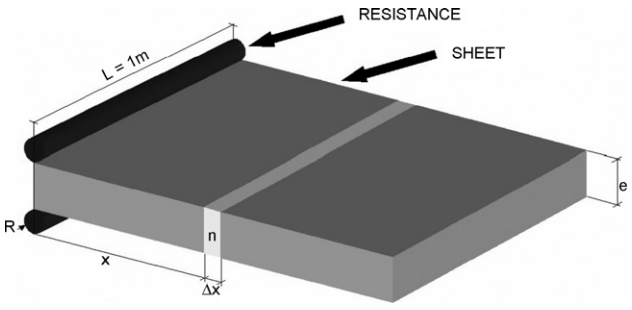

Fig. 2 – Scheme of thermal model.

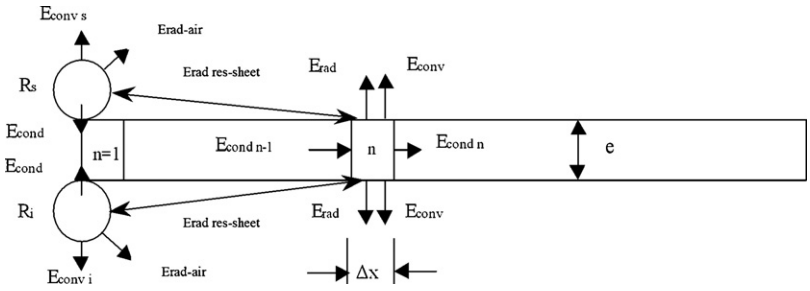

Fig. 3 – Thermal flows in element *n*.

In element $n = 1$ conduction flows with resistances should also be considered.

In resistances convection and radiation flows to air should be taken into account.

2.1. *Temperature in element n*

With this assumptions expression of temperature in element n, in time t is given by the following equation:

$$T(t)_n = T(t-1)_n + \frac{\Delta E_{cond} - \Delta E_{conv} - \Delta E_{rad} + \Delta E_{radres\text{-}sheet1} + \Delta E_{radres\text{-}sheet2}}{C(T(t-1)_n)\rho_{sheet}\Delta x\, e}\Delta t \quad (1)$$

being ρ_{sheet} material density, $C(T)$ specific heat (dependent on temperature).

Energy increment (in each time unit) due to conduction flows is

$$\Delta E_{cond} = \frac{k(T(t)_n)e}{\Delta x}(T(t)_n - T(t)_{n-1}) - \frac{k(T(t)_{n+1})e}{\Delta x}(T(t)_{n+1} - T(t)_n) \quad (2)$$

being $k(T)$ thermal conductivity (dependent on temperature).

Energy decrement (in each time unit) in element n due to convection flow to air is

$$\Delta E_{conv} = \Delta x(T(t)_n - T_{room})(\bar{h}_{sup} + \bar{h}_{inf}) \quad (3)$$

being $\bar{h}_{sup}$ and $\bar{h}_{inf}$ convection heat transfer coefficients in both surfaces of the sheet, and T_{room} room temperature.

Energy decrement (in each time unit) in element n due to radiation from element to air is

$$\Delta E_{rad} = 2\Delta x\varepsilon_{sheet}\sigma(T(t)_n{}^4 - T_{room}^4) \quad (4)$$

being ε_{sheet} sheet emissivity.

Energy increment (in each time unit) in element n due to radiation from resistances:

$$\Delta E_{radres-sheet1} = \Delta E_{radres-sheet2} = \Delta x\varepsilon_{res}F_{r-s}\sigma(T_{res}^4 - T(t)_n{}^4) \quad (5)$$

being ε_{res} resistance emissivity, and F_{r-s} view factor dependent on element geometry. A way to calculate this parameter can be found in Incropera and De Witt (1999).

2.2. *Resistances temperature*

Firstly, initial temperature in resistances (before contact with sheet) should be calculated as a function of heating parameters. Total power in resistances is dissipated in radiation and convection. Relation between radiation power (W_{rad}) and convection power (W_{conv}) and temperature in resistances is

$$W = W_{rad} + W_{conv} = 2\pi R[\sigma\varepsilon_{res}(T_{res}^4 - T_{room}^4) - \bar{h}(T_{res} - T_{room})] \quad (6)$$

Equation is solved with iterative Newton method.

Resistances were put in contact with first element, so contact thermal resistance between resistances and sheet should be established. During heating time, contact resistance varies, because it depends on contact force and contact area, and last parameter depends on temperature. These parameters were established taking into account previous finite element study. From experimental work (Canteli, 2003) contact thermal resistance was established as follows:

$$R = (3t^2 - 116t + 1125)\frac{1650 - P}{35,000} + 113.16\,e^{0.1497t} + (5t^3 - 185t^2 + 1750t + 3250)\frac{562.5 - a}{187,500} \quad (7)$$

being t heating time, P power resistance and a contact force.

Energy increment in first element is

$$\Delta E_{cond} = \frac{1}{R}\frac{\delta}{2}(T_{res} - T_0) \quad (8)$$

being δ contact area and T_0 initial temperature in first element.

Resistances temperature is calculated as

$$T(t)_n^{res} = T(t-1)_n^{res} + \frac{w - \Delta E_{cond} - \Delta E_{conv} - \Delta E_{rad-air} - \Delta E_{rad-sheet}}{C(T(t-1)_n^{res})\rho_{res}\pi(R^2/2)} \quad (9)$$

Energy decrement in resistances because of radiation to sheet ($\Delta E_{rad-sheet}$) and air ($\Delta E_{rad-air}$), and convection to air (Churchil and Chu, 1975) (ΔE_{conv}) could be established as follows:

$$\Delta E_{rad-air} = \pi R F_{res\text{-}air}\varepsilon_{res}\sigma(T_{res}^4 - T_{room}^4) \quad (10)$$

being R resistance radius, $F_{\text{res-air}}$ view factor (in this case 0.5), σ Stefan–Boltzmann constant (5.67×10^{-8} W/m^2 K^4).

$$\Delta E_{\text{rad–sheet}} = \Delta x \varepsilon_{\text{res}} \sigma \sum_n F_{\text{r-s}}(n)(T_n^4 - T_{\text{res}}^4) \tag{11}$$

$$\Delta E_{\text{conv}} = \pi R \bar{h} k_R (T_{\text{res}} - T_{\text{room}}) \tag{12}$$

being $\bar{h}$ convection heat transfer coefficient of resistance.

Eqs. (1)–(12) are used to calculate temperature distribution in sheet and resistances at each time value. Time interval was selected according to stability requirements. Stability criterion (Incropera and De Witt, 1999) is in this case,

$$1 - 2Fo \geq 0, \tag{13}$$

where Fo is Fourier number,

$$Fo = \frac{\alpha \Delta t}{(\Delta x)^2} \tag{14}$$

that implies $Fo \leq (1/2)$ and being

$$Fo = \frac{\alpha \Delta t}{\Delta x^2} \tag{15}$$

so it is deduced:

$$\Delta t \leq \frac{\Delta x^2}{2\alpha} = \frac{(\Delta x)^2 \rho c_p}{2k} \tag{16}$$

Time values are fixed in order to obtain permanent temperature distributions. The choice of Δx is based on a compromise between accuracy and computational requirements.

Once temperature distribution is obtained, it is possible to determinate mechanical properties in each element. Parameters of constitutive equation are a function of temperature.

Thermo-mechanical model will be validated with stainless steel AISI 304. Temperature dependence of constitutive equation parameters was established from experimental work. A large number of tests were carried out in order to obtain stress–strain curve parameters of this material, from room temperature to temperatures up to 770 °C. From these tests constitutive equation parameters $E(T)$, $\sigma_{0e}(T)$, $K_e(T)$ (see Fig. 4) were obtained as a function of temperature.

Mechanical behaviour of AISI 304 at high temperature is represented by a coefficient (temperature dependent) that multiplies parameter values at room temperature. Dependence of these parameters with temperature is represented in Fig. 5. Curves were adjusted by fifth and fourth order polinomials in T.

3. Bending model formulation

Air bending model is schematically represented in Fig. 6. An equivalent problem to actual bending process, symmetrical with respect to bending plane YZ is represented. Middle section of the sheet is attached and the force due to contact between die and sheet is applied in contact point (X_k, Y_k).

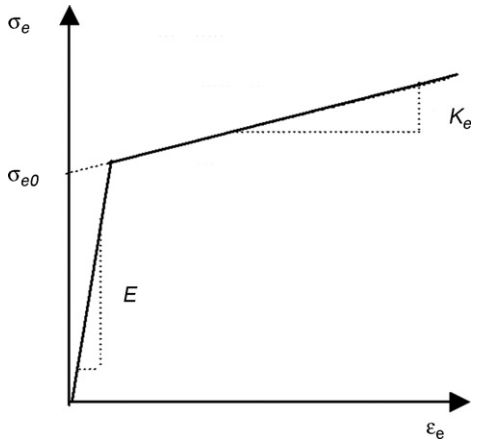

Fig. 4 – Parameters of constitutive equation of material sheet.

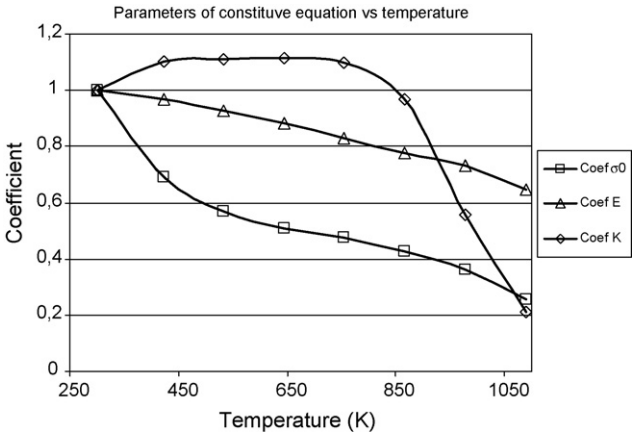

Fig. 5 – Coefficients of parameters of constitutive equation versus temperature.

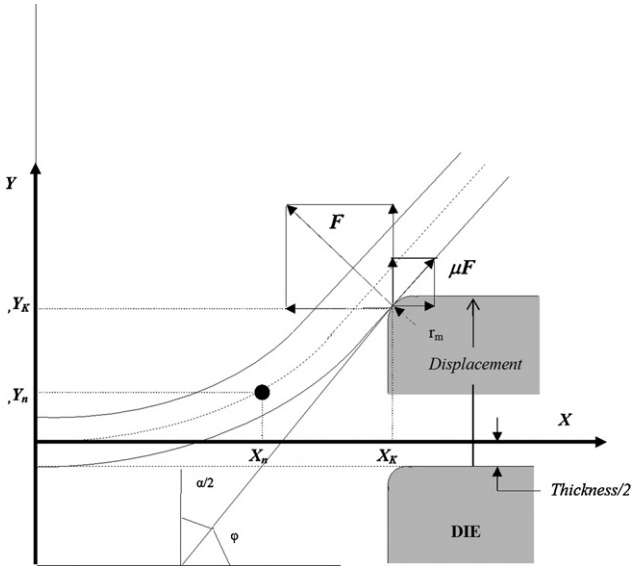

Fig. 6 – Scheme of analytical model of air bending process.

The sheet is discretized in elements Δx width, 1 m length, and e thick, in the same way as it was done in thermal model.

Several hypotheses are assumed:

- During punch displacement, reaction force between die and sheet F, varies, in module and direction, as the sheet is being bent. Point of application of this force in the sheet varies too.
- Effective die aperture (position of contact point) varies as the sheet is being bent.
- Friction between sheet and die is taken into account.

3.1. *Equilibrium conditions*

Moment in a generic element n with central point coordinates (X_n, Y_n) is given by

$$M_n = F\{(\sin\varphi - \mu\cos\varphi)(Y_k - Y_n) + (\cos\varphi + \mu\sin\varphi)(X_k - X_n)\} \quad (17)$$

where μ is friction coefficient between sheet and die, (X_k, Y_k) the co-ordinates of sheet–die contact point, F the normal force due to this contact and φ is the angle related to bending angle α as follows:

$$\varphi + \frac{\alpha}{2} = \frac{\pi}{2} \quad (18)$$

This external moment should be in equilibrium with internal moments. Internal moment for bending without tension is calculated with several assumptions (Marciniak and Duncan, 1992). In thin sheets, normal section planes may be considered to remain plane on bending and to converge on the centre of curvature as illustrated in Fig. 7, representing a generic element n. Constant curvature is assumed in each element.

It is also considered that the principal directions of stress and strain coincide with the radial and circumferential directions, so that there is no shear in the radial plane and gradients of stress and strain are zero in the circumferential direction. Middle surface is not deformed. As bend length is large compared with thickness, plane strain conditions are assumed.

With these assumptions (see Fig. 7) engineering strain is calculated as shown in Eqs. (19)–(21). Subscript 0 denotes magnitudes in middle surface (R_0 is radius in middle surface) and x, y, z are local axis in element n,

$$L_0 = R_0\theta \quad (19)$$

$$L = (R_0 + y)\theta \quad (20)$$

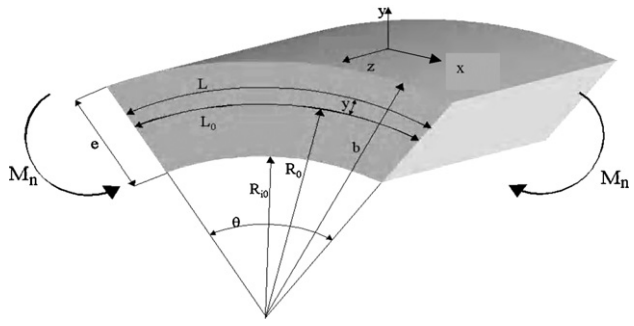

Fig. 7 – Curvature and strains in a sheet element during bending.

$$e_x = \frac{L - L_0}{L_0} = \frac{y\theta}{R_0\theta} = \frac{y}{R_0} \quad (21)$$

So, true strain is

$$\varepsilon_x = \ln\left(\frac{1+y}{R_0}\right) \cong \frac{y}{R_0} \quad (22)$$

From Levy–Mises equations (increasing monotonic load is considered) effective strain and stress (ε_e, σ_e) are calculated (Timoshenko, 2002):

$$\varepsilon_e = \frac{2\varepsilon_x}{\sqrt{3}} \quad (23)$$

$$\sigma_e = \frac{\sigma_x\sqrt{3}}{2} \quad (24)$$

Moment equilibrium in element n implies:

$$M_n = \int_{-e/2}^{+e/2} \sigma_x y\,dy \quad (25)$$

In this equation σ_x is related with σ_e and so with ε_e, by material constitutive equation.

3.2. *Constitutive equation*

Validation of the model was carried out with stainless steel AISI 304. An elastic–plastic model with linear strain hardening was selected according to previous mechanical characterization of this material. Temperature dependence of constitutive equation parameters (see Fig. 4) elastic modulus $E(T)$, $\sigma_{0e}(T)$ and $K_e(T)$) was analysed in previous section.

In elastic region, constitutive equation is

$$\sigma_e = E\varepsilon_e \quad (26)$$

and in elasto-plastic region

$$\sigma_e = \sigma_{0e} + K_e\varepsilon_e \quad (27)$$

Taking into account these considerations and Eqs. (22)–(24), equation for σ_x in elastic region, could be written as

$$\sigma_x = \frac{E\varepsilon_x}{1-\nu^2} = \frac{Ey}{(1-\nu^2)R_0} \quad (28)$$

where ν is Poisson coefficient.

In elasto-plastic region equation for σ_x is

$$\frac{\sqrt{3}}{2}\sigma_x = \sigma_{0e} + \frac{2K_e\varepsilon_x}{\sqrt{3}} \quad (29)$$

and so

$$\sigma_x = \frac{2\sigma_{0e}}{\sqrt{3}} + \frac{4K_e\varepsilon_x}{3} = \frac{2\sigma_{0e}}{\sqrt{3}} + \frac{4K_e y}{3R_0} \quad (30)$$

From Eqs. (28), (30) and (25) the bending moment can be expressed as follows:

$$M_n = 2\left[\int_0^{\varepsilon_x^* R_0} \frac{E}{1-\nu^2}\frac{y^2}{R_{0n}}dy + \int_{\varepsilon_x^* R_0}^{e/2} \frac{2}{\sqrt{3}}\sigma_{0e} + \frac{4K_e}{3}\frac{y}{R_{0n}}y\,dy\right] \quad (31)$$

where integration limits in equation are given by the point where yielding begins, corresponding to strain given in the following equation:

$$\varepsilon_x^* = \frac{\sigma_{0e}(1-\nu^2)}{(E-K_e)\sqrt{1-\nu+\nu^2}} \quad (32)$$

Integration of Eq. (31) relates M_n with curvature R_{0n} in element n:

$$M_n = (R_{0n}\varepsilon_x^*)^2\left[\frac{2}{3}\varepsilon_x^*\left(\frac{E}{1-\nu^2}-\frac{4}{3}K_e\right)-\frac{2}{\sqrt{3}}\sigma_{0e}\right] + 0.2887\sigma_{0e}e^2 + \frac{K_e e^3}{9R_{0n}} \quad (33)$$

As constitutive equation parameters ($E(T)$, $\sigma_{0e}(T)$, $K_e(T)$) depends on temperature, Eq. (33) should be formulated once temperature in each element is calculated, as was explained in second paragraph.

Moment calculated from Eq. (33) should be equal to moment deduced from external forces given in Eq. (17).

3.3. *Relation between curvature and Y(X)*

Eq. (34) relating curvature in each element and Y(X) is given by Marciniak and Duncan (1992):

$$\frac{1}{R_{0n}} = \frac{(d^2Y/dX^2)_n}{[1+(dY/dX)_n^2]^{3/2}} \quad (34)$$

Final curvature after unloading $1/R_{fn}$ is calculated as

$$\frac{1}{R_{0n}} - \frac{1}{R_{fn}} = \frac{M_n}{Ee^3/12(1-\nu^2)} \quad (35)$$

and final Y(X) of the sheet (in each element n) after unloading, is related to final curvature as follows:

$$\frac{1}{R_{fn}} = \frac{(d^2Y/dX^2)_n}{[1+(dY/dX)_n^2]^{3/2}} \quad (36)$$

4. Solution

In a first step R_0^*, radius where yielding occurs in $y=\pm(e/2)$, is calculated as follows:

$$R_0^* = \frac{e\sqrt{3}}{4\sigma_{0e}}\left(\frac{E}{1-\nu^2}-\frac{4}{3}K_e\right) \quad (37)$$

As it has been shown, moment resulting from external forces is calculated (Eq. (17)). Note that F, φ, X_k, Y_k are not known, these parameters should be arbitrarily fixed, as a first step of the iterative process.

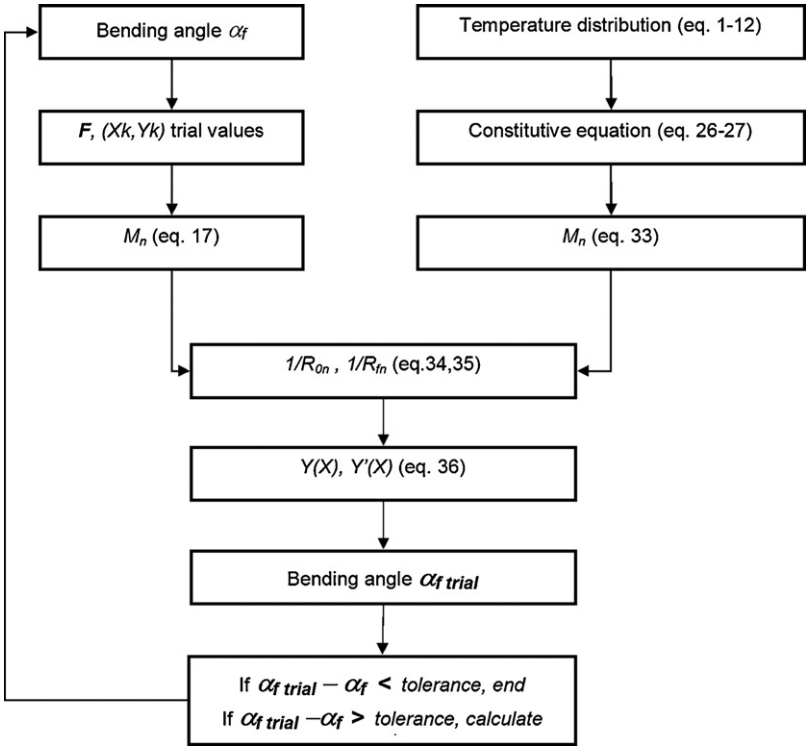

Fig. 8 – Scheme of solution steps.

This moment in element n, should be equal to internal moment resulting from Eq. (33). Newton method (Bilal and McCuen, 1996) is used to calculate R_{0n} from this equation. If $R_{0n} < R_0^*$ (elasto-plastic) then R_{0n+1} is calculated in a similar way. If $R_{0n} \geq R_0^*$ (elastic) then R_{0n} is recalculated as

$$R_{0n} = \frac{E}{1-\nu^2}\frac{1}{M_n}\frac{e^3}{12} \tag{38}$$

This calculation process relates external forces with moments at each element and moments with curvature. Principal disadvantage of the process derive from the fact that moment at each point is a function of its own co-ordinates, contact point coordinates and contact angle at this point. However, these parameters are not known. When a force is applied, resulting sheet displacement is not known, and so, function Y(X), contact point coordinates, and contact force direction are not known.

From Eq. (34) Y(X) and its derivatives are obtained. Boundary conditions are $Y=0$ and $dY/dX=0$ in $X=0$, and solving method is 4th order Runge–Kutta (Hultquist, 1988).

Then, bending angle before springback, is calculated. When unloading occurs, final curvature in each point after springback is calculated as

$$\frac{1}{R_{fn}} = \frac{1}{R_{0n}} - \frac{12(1-\nu^2)M_n}{Ee^3} \tag{39}$$

and relation between curvature and final Y(X) is given by Eq. (36). This equation is also solved by a 4th order Runge–Kutta method with contour conditions $Y=0$ and $dY/dX=0$ in $X=0$. Bending angle after springback is calculated. Differences between estimated and calculated values indicate if it is necessary to iterate again.

Summarizing, once desired bending angle is established, moment at each point is calculated, assuming initial values of F and (X_k, Y_k) arbitrarily determined. After, curvature is determined, as explained previously. Y(X) and derivatives are obtained from curvature, before and after unloading. Differences between established and calculated bending angle indicate if it is necessary to calculate again. The procedure is stopped once a convergence criterium is reached. Solution method is represented in Fig. 8.

5. Results and discussion

After establishment of heating parameters, temperature distribution in each element as a function of heating time is calculated with thermal model. Heating parameters range between values that are determined from projected experimental device. Contact force ranges from 375 to 750 N/m. Resistance power ranges from 900 to 2000 W/m. Sheet thickness varies from 2 to 6 mm. Heating device, was designed for low cost and easy implementation in industrial processes.

Fig. 9 shows temperature evolution (up to 5 min) in several elements, sheet thickness was 4 mm, resistance power was 2000 W/m and contact force was 750 N. As FEM simulation showed previously, permanent conditions were reached before 20 min, even when thickest sheet is heated. Temperatures up to 770 °C were reached corresponding to maximum contact force and resistances power.

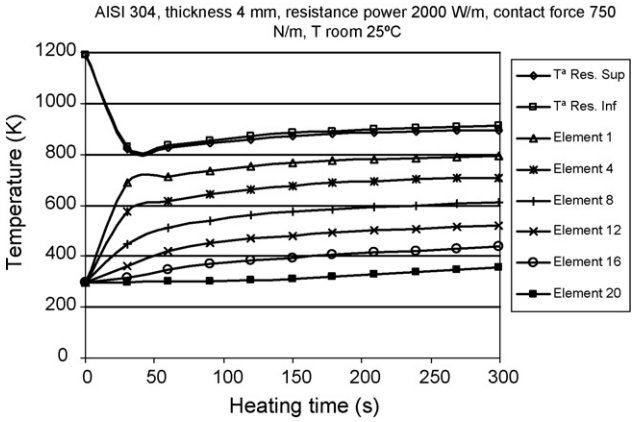

Fig. 9 – Temperature evolution in elements 1–20 and resistances.

Fig. 10a shows temperature distribution in two extreme cases: high power and high contact force (temperatures up to 770 °C are reached) and low power and low contact force (temperatures up to 580 °C). Fig. 10b shows steady temperature

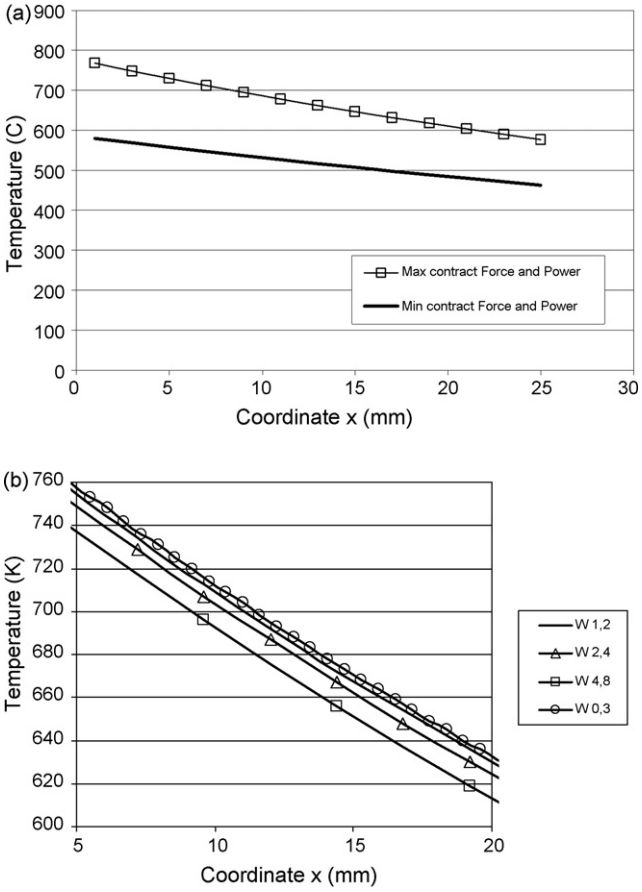

Fig. 10 – (a) Extreme temperature distributions corresponding to maximum and minimum contact force and resistance power. (b) Influence of element width in temperature distribution.

distribution in a sheet with different element width. Curves of temperature versus x co-ordinate are not very different, however time of calculation increases hardly when element width decreases. The element width was stated as a compromise between accuracy and time of calculation.

Bending model is formulated in order to satisfy industrial requirements. Desired geometry of the piece fixes final bending angle after unloading, being this parameter the input of the model. An iterative calculation process allows solving equations presented in Section 3, obtaining curvature, equation $Y(X)$ and its derivatives, and contact force. These parameters are very important in an industrial process, for the establishment of punch displacement and maximum force to make the piece.

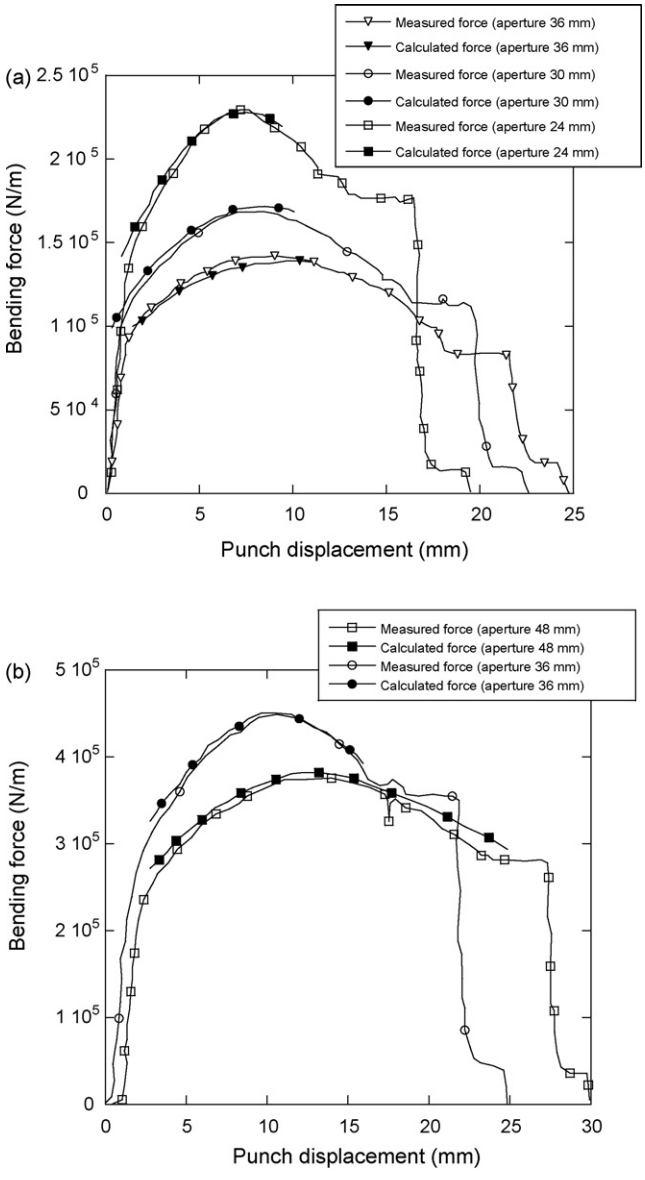

Fig. 11 – (a) Measured and calculated bending force at room temperature versus punch displacement, sheet thickness 3 mm, die aperture 24, 30 and 36 mm. (b) Measured and calculated bending force with high temperature distribution (max. 770 °C) versus punch displacement, sheet thickness 6 mm, die aperture 48 and 36 mm.

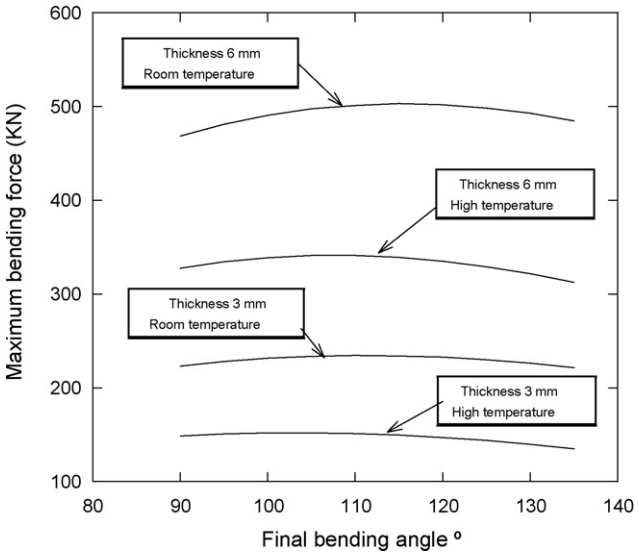

Fig. 12 – Influence of temperature in calculated bending force at room and with high temperature distribution. Sheet thickness 3 mm (room temperature and 580 °C) and sheet thickness 6 mm (room temperature and 770 °C).

Validation of the model was carried out comparing calculated and experimental bending forces in several cases (sheet thickness, die aperture, room and high temperature). Experimental tests were carried out in the experimental device designed and constructed to validate the model (Canteli et al., 2006). In Fig. 11a measured and calculated bending force at room temperature versus punch displacement is shown. The forces correspond with sheet thickness 3 mm and die aperture 24, 30 and 36 mm. In Fig. 11b measured and calculated bending force with high temperature distribution (max. 770 °C) versus punch displacement is shown. The tests and calculations shown in this figure correspond with sheet thickness 6 mm and die aperture 36 and 48 mm. There is a elevated correspondence between experimental and predicted forces, both at room and high temperature. Error was calculated as relative difference between analytical and experimental values, and it was less than 5% in every case.

The model was used to evaluate the influence of temperature in maximum bending force. In Fig. 12, calculated maximum bending force at room temperature and with two temperature distributions: up to 580 °C, and up to 770 °C are presented. Important decrease in bending force (33%) is predicted for maximum temperature in both cases.

Other results can be obtained from this model: maximum stress and strain. These results are related to important features of the industrial process, like tools design and formability limits of the sheet. Fig. 13a and b present respectively maximum stress and strain calculated with the model, with sheet thickness 4 mm, die aperture 32 mm. In both figures, results when the distributed temperature is considered (obtained form thermal model, maximum value 770 °C) and when a uniform temperature is considered (constant temperature equal to 770 °C), are presented. The hypothesis of constant maximum temperature leads to underestimated stresses and strains that could be significant in a workpiece

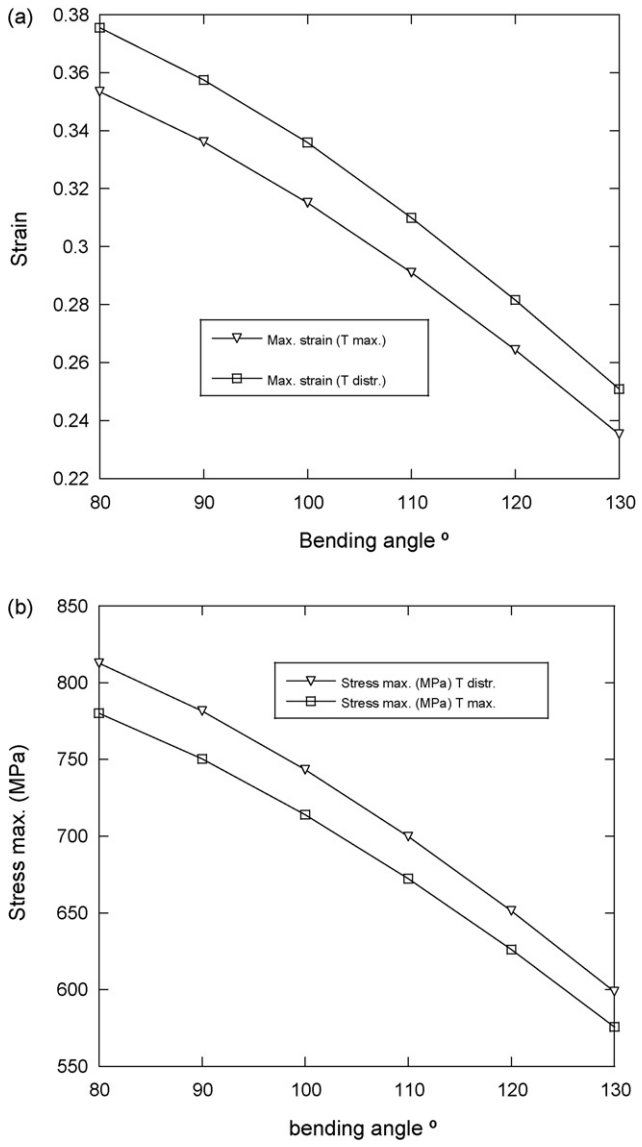

Fig. 13 – (a) Maximum calculated strain in the sheet, when a distribution of temperature (max. 770 °C) and uniform temperature (770 °C) is assumed. Sheet thickness 4 mm, die aperture 32 mm. (b) Maximum calculated stress in the sheet, when a distribution of temperature (max. 770 °C) and uniform temperature (770 °C) is assumed. Sheet thickness 4 mm, die aperture 32 mm.

with a shape that impose strain and stress close to the limit of formability.

These results give important information concerning the state of the sheet material. Maximum stress and maximum strain permissible in the material would fix the punch displacement allowable. On the other hand, the prediction of the springback is crucial to determine the final geometry of the piece. It is clear the utility of the model because those parameters are difficult to evaluate and measure during bending process.

The model presented in this paper allows calculating temperature distribution in the sheet, bending force and springback, once the process parameters are defined. The CPU time was only few seconds; a clear advantage compared with that involved in a FEM analysis of bending at high temperature, carried out in a FEM code.

6. Conclusions

The principles of a model for air bending process at local elevated temperature have been analysed. Temperature distribution is calculated taking into account heating parameters of the designed heating device for experimental validation. This heating device was designed based in not expensive technologies, easy to implement in industrial processes.

Bending model does not assume a previous sheet shape, as occurs in actual process. Equation Y(X) given the shape of the sheet is obtained in an iterative calculation process, being the bending angle the input of this process. This model take into account mechanical properties as a function of temperature, once temperature distribution is calculated from the thermal model.

This work would help to implement in industry bending process at high temperature, when it was necessary, or would improve bending parameter predictions, at room temperature. Accuracy of the model was proven comparing calculated and measured bending force, with error less than 5%.

REFERENCES

Anokye-Siribor, K., Singh, U.P., 2000. A new analytical model for pressbrake forming using in-process identification of material characteristics. J. Mater. Process. Technol. 99, 103–112.

ANSYS, 2000. ANSYS User Manual.

Asnafi, N., 2000. Springback and fracture in v-die air bending of thick stainless steel sheets. Mater. Des. 21, 217–236.

Bilal, M.A., McCuen, R.H., 1996. Numerical Methods for Engineers. Prentice-Hall International, Londres.

Canteli, J.A., 2003. Air Bending Process of Stainless Steel with Local Heating. PhD Thesis. University Carlos III of Madrid.

Canteli, J.A., Cantero, J.L., Miguélez, M.H., 2006. Development of software for easy prediction of process parameters in air bending with local heating. Int. J. Vehicle Des. 42, 170–197.

Churchil, S.W., Chu, H.H.S., 1975. Correlating equations for laminar and turbulent free convection from a horizontal cylinder. Int. J. Heat Mass Transfer 18, 1049.

de Vin, L.J., 2000. Curvature prediction in air bending of metal sheet. J. Mater. Process. Technol. 100, 257–261.

de Vin, L.J., 2001. Expecting the unexpected, a must for accurate brake forming. J. Mater. Process. Technol. 117, 244–248.

de Vin, L.J., Streppel, A.H., Singh, U.P., Kals, H.J.J., 1996. A process model for air bending. J. Mater. Process. Technol. 57, 48–54.

Hsu, C.W., Ulsoy, A.G., Demeri, M.Y., 2002. Development of process control in sheet metal forming. J. Mater. Process. Technol. 127, 361–368.

Hultquist, P.F., 1988. Numerical Methods for Engineers and Computer Scientists. Benjamin-Cummings, Cop., Menlo Park.

Incropera, F.P., De Witt, D.P., 1999. Fundamentals of Heat and Mass Transfer. Addison Wesley Longman, p. 827.

Marciniak, Z., Duncan, J., 1992. Mechanics of Sheet Metal Forming. Edward Arnold, Londres.

Timoshenko, 2002. Resistencia de Materiales. Thomson, Madrid.